Nano-magnesium oxide reinforced polylactic acid biofilms for food packaging applications

Chetan Swaroop, Mukul Shukla

PII: S0141-8130(18)30303-9
DOI: doi:10.1016/j.ijbiomac.2018.02.156
Reference: BIOMAC 9213

To appear in:

Received date: 19 January 2018
Revised date: 20 February 2018
Accepted date: 26 February 2018

Please cite this article as: Chetan Swaroop, Mukul Shukla , Nano-magnesium oxide reinforced polylactic acid biofilms for food packaging applications. The address for the corresponding author was captured as affiliation for all authors. Please check if appropriate. Biomac(2017), doi:10.1016/j.ijbiomac.2018.02.156

Nano-Magnesium Oxide Reinforced Polylactic Acid Biofilms for Food Packaging Applications

Chetan Swaroop [a,*], Mukul Shukla [a, b]

[a] Mechanical Engineering Department, Motilal Nehru National Institute of Technology, Allahabad, India

[b] School of Mechanical and Aerospace Engineering, Faculty of Engineering and Physical Sciences, Queen's University, Belfast, UK

[*]Corresponding author: chetanswaroop019@gmail.com

Abstract

This study is aimed at producing biofilms by reinforcement of Magnesium Oxide (MgO) nanoparticles in polylactic acid (PLA) biopolymer using the solvent casting method. In this study MgO nanoparticles (up to 4 wt%) were reinforced in PLA biopolymer and their key mechanical, barrier, thermal and antibacterial properties were investigated for food packaging applications. Among the prepared biocomposite films, the 2 wt% reinforced PLA films showed the maximum improvement in tensile strength and oxygen barrier properties (up to 29% and 25% respectively) in comparison to pristine PLA films. However, the water vapour barrier properties decreased by nearly 25% due to interfacial behaviour and presence of free volumes near MgO nanoparticles. PLA/MgO films also exhibited superior antibacterial efficacy. The 2 wt% biofilms caused progressive damage and death of nearly 46% of E. Coli bacterial culture after 12 h treatment. The produced films are transparent, capable of screening UV radiations and exhibit superior antibacterial efficacy making them an excellent food packaging material.

Keywords

PLA films; MgO nanoparticles; Biofilms; food packaging; barrier properties; tensile properties

1. Introduction

Polymers ease the achievement of essential packaging functions such as protection and preservation of goods along with convenience in delivery and consumption. Polymers are well regarded for their high strength to weight ratio which encourages their application over metals or glass, particularly in packaging applications. However, rapid consumption of petroleum-based polymers has given rise to global litter production, mainly due to its slow rate of degradation and lack of strategic recycling and discarding facilities [1]. During previous decades researchers have investigated a number of biopolymers to address the demerits of petroleum-based polymers. Polylactides, chitosan, polyhydroxy alkenoates, starches etc. are few popular biopolymers which are extensively being studied for their utilization as a sustainable packaging material. However, despite their superior properties they have their own limitations, including high moisture affinity, low thermal stability, poor barrier properties and heat sealability [2, 3].

Among the various biopolymers investigated, polylactic acid (PLA) has emerged as the most promising biopolymer owing to its biodegradability, renewability and superior mechanical properties. PLA is mainly produced by condensation polymerization from lactic acid, derived by fermentation of sugars, corn, sugarcane, or tapioca. The key properties of PLA such as degradation, crystallization and process ability depends largely on ratio of the L/D-isomer of lactic acid [2]. However, PLA also suffers from the above drawbacks which restrict its direct utilization in packaging applications [2, 3].

To overcome these issues of PLA different approaches have been adopted such as addition of plasticizers, polymer blending, coupling agents, co-polymerization and nanotechnology [4-6]. Many researchers have advocated utilization of nanotechnology due to its multi-folded benefits in addition to mitigation of various short comings of PLA [4]. Recent research highlighted that among wide-ranging nanofillers, reinforcement of metal oxides in polymer matrix offers improved antibacterial and ultraviolet (UV) screening properties, in addition to the improved mechanical and barrier properties. These additional features help in improving the shelf life of packaged food. Addition of metal oxides, such as ZnO, MgO, TiO_2 and SiO_2 into different polymer matrices are recently being studied for their potential use as a packaging material [2, 4, 8]. Among these metal oxides, Magnesium Oxide (MgO) occurs naturally as a reproducible, colourless, crystalline mineral and can be economically produced in large-scale [9]. Furthermore, U. S. Food and Drug Administration (FDA) also recognizes the use of MgO, as generally safe even for food applications. The antibacterial efficacy and UV screening ability of produced PLA/MgO biopolymer films was previously presented by the authors [10]. Considering the above cited attributes, the reinforcement of MgO nanoparticles in PLA seems to be a prospective approach for food packaging applications.

To the best of our knowledge, so far there is no study reported on the mechanical, thermal and barrier properties of PLA/MgO biocomposite films. This study is focused on the development of PLA/ MgO films and its assessment for food packaging applications. Essential properties such as tensile, thermal, gas and water vapour barrier properties and antibacterial efficacy of PLA/MgO biofilms were investigated. The generated

information is likely to prove valuable in establishing PLA/ MgO biofilms as a sustainable food packaging material option.

2. Experimental

2.1. Material

Commercially available PLA (Ingeo 4043D resin) of melting temperature 145-160°C was procured from NatureWorks LLC, USA in pellet form and used in this research. The 99.9% purity MgO nanopowder was supplied by Nanoshel LLC, USA. The white in colour nanopowder of 40.3 g/mol molecular weight had a polyhedral morphology and an average particle size of less than 60 nm. Chloroform used as a solvent was procured from Fisher Scientific (India) Pvt. Ltd., Mumbai, India.

2.2. Preparation of biofilms

In this study, PLA/ MgO films with 1, 2, 3 and 4 weight percent (wt%) compositions (henceforth referred to as P1, P2, P3 and P4 respectively throughout the text) were prepared by the commonly used solvent casting method using chloroform as the solvent. PLA resin has high moisture affinity, therefore, PLA pellets were dried at first at 60°C for 24 h, before dissolving in chloroform. 5 g of dried PLA was dissolved in 50-55 ml chloroform by vigorous stirring of around 3 h with the help of a magnetic stirrer. MgO nanoparticles (NPs) were accurately weighed to obtain the desired composition and dispersed separately in chloroform with the help of a 40 kHz ultrasonicator for 15 minutes and then poured in to the dissolved PLA solution and continued to stir for one more hour for better dispersion. The obtained mixture of MgO NPs suspended in

dissolved PLA matrix was evenly spread at room temperature on a glass plate with the help of a bird type manual film applicator allowing evaporation of chloroform to produce uniform thickness films, in comparison to the films produced by the popularly used petri dish method. After 2-3 days, dried films were peeled out from the plate and stored in a dry place. The peeled-out films were conditioned at 45°C for 24 h to remove any residual solvent acting as a plasticizer. The thickness of prepared films was found between 35-45 µm as measured using a handheld electronic micrometer (least count 1 µm). Pristine PLA films were also prepared similarly without loading MgO NPs (referred as P0 hereafter). The different types of as-prepared films are shown in Fig. 1. It can be well established from the figure that the prepared films demonstrate good transparency (minimum 86% for 4 wt% films).

Figure 1: Different types of prepared biofilms: (P0) Neat PLA, (P1) 1 wt%, (P2) 2 wt%, (P3) 3 wt% and (P4) 4 wt% PLA/MgO biofilms

3. Characterizations and testing

The chemical structure of the prepared films was investigated by FTIR analysis. The FTIR spectra of PLA and PLA/MgO films were recorded in the range of 4500–650 cm^{-1} using a Perkin Elmer (Spectrum 100 Series) spectrophotometer. The crystallographic properties of MgO nanopowder and prepared biofilms were studied by X-ray diffraction (XRD) using a Rigaku Smartlab (3 KW) instrument. The samples were scanned from 5° to 65° at the rate of 5° per minute. The surface morphology and element mapping of the prepared films were investigated by capturing micrographs of the representative samples using Nova Nano SEM 450, a field-emission scanning electron microscope (FE-SEM)

equipped with energy-dispersive X-ray (EDX) analyzer. The samples of the prepared films were prior coated with gold for 2 minutes using an EMITECH SC7620 Mini Sputter Coater.

The tensile strength of PLA/MgO biocomposite films was found out using a Tinius-Olsen universal testing machine (UTM). The UTM was equipped with a 250 N load cell and rubber lined flat grips. The specimens were cut into rectangular strips of 150 x 10 mm^2 size following the ASTM D882-2002 standard. The tensile tests were conducted at a strain rate of 10 mm/min in 70% RH and 30°C surrounding conditions. Four specimens of each composition were tested and average of the thicknesses measured at five distinct locations along the length of the specimens was used to compute the stress.

Thermal properties of the PLA/MgO films were studied by differential scanning calorimetry (DSC) and thermo-gravimetric analysis (TGA) analysis. DSC was undertaken using a Perkin Elmer DSC 6 instrument. The samples were scanned in nitrogen gas environment from room temperature to 170°C at a heating rate of 5°C/min with a 5 min isotherm at 170°C followed by cooling to room temperature at the same rate. The samples were reheated from room temperature to 170°C at 5°C/min in the same environment to erase the thermal history of samples. TGA was performed on a Perkin Elmer TGA 4000 instrument with around 10 µg of each sample by heating from room temperature to 600°C in nitrogen gas environment.

Gas barrier property of the prepared films was studied against permeability of oxygen gas. The oxygen transmission rate (OTR) was obtained using N500-GBPI Packaging Test Equipment, according to ASTM D1434-82 standard. All the tests were

performed at 23°C temperature and 53% RH. The permeability of films was computed with the help of the following relation:

$$OP = OTR \times (t/\Delta p)$$

where OP is oxygen permeability, t is thickness of the film and Δp is partial pressure difference across two sides of the film.

Water vapor transmission rate (WVTR) of prepared films was measured according to modified ASTM E 96-95 method. Circular samples of 14 cm diameter, were wrapped around the stainless-steel water vapor permeability measuring cups. The cups were filled with distilled water around 2.5cm below the film surface and kept in a chamber at 29°C and 70% RH. The cups were weighed every 24 h up to 72 h and the WVTR was measured. Water vapor permeability (WVP) of prepared films was calculated using the following relation:

$$WVP = WVTR \times t/\Delta p$$

where t is average film thickness and Δp is partial water vapor pressure difference across the two sides of the film.

Antibacterial efficacy of the prepared biofilms was studied against E. Coli (a foodborne bacteria) culture by using the Fluorescence Activated Cell Sorting (FACS) technique with the help of BD ACCURI C6 flow cytometer. Methodology for growth of the bacterial culture and preparation of FACS sample were adopted from [11]. A total of 10,000 events were acquired for each sample and the BDC6 sampler software package

was used to analyze the results. The E. Coli culture was treated with 5 x 5 cm^2 samples of PLA and PLA/MgO biofilms.

4. Results and discussion

4.1. Characterization of PLA and PLA/MgO biofilms

To establish the interaction between PLA matrix and MgO nanofiller FTIR analysis was performed. The transmission spectra of PLA and PLA/MgO films is illustrated in Fig. 2.

Figure 2: FTIR spectra of prepared films: Neat PLA (P0), 1 wt% (P1), 2 wt% (P2), 3 wt% (P3) and 4 wt% (P4) PLA/MgO biofilms

The absorption bands of the recorded spectra were matched with previous literature [12, 13] and the prominent bands observed are included here. The small transmittance peaks corresponding to 2996 and 2946 cm^{-1} can be attributed to asymmetric and symmetric stretching of the CH_3, while the signal near 2880 cm^{-1} belongs to C—H stretching. The C=O stretching generates a strong signal, captured near 1760 cm^{-1}. The IR bands around 1453, 1383 and 1361 cm^{-1} are assigned to the —CH— deformation including symmetric and asymmetric bending. The C—O stretching of the ester group appears at 1267 cm^{-1}. The signal at 956 cm^{-1} appears due to the rocking mode of CH_3. The FTIR investigation reveals that substantial peaks of PLA and its biocomposite films occur at same positions. Furthermore, observation of no significant new peak indicates that the MgO NPs have a physical interaction only with PLA instead of any chemical bonding which apprises the successful preparation of biocomposite films [14].

The crystallographic structure of polymers plays a vital role in interpreting the key mechanical, barrier and thermal properties. Hence, it becomes important to study the crystallographic properties of the prepared biofilms. The XRD patterns of the MgO NPs and PLA/MgO biofilms are illustrated in Fig. 3.

Figure 3: XRD diffractograms of MgO NPs and prepared biocomposite films: (P0) Neat PLA, (P1) 1 wt%, (P2) 2 wt%, (P3) 3 wt% and (P4) 4 wt% PLA/MgO biofilms

The diffractograms of MgO nanopowder exhibit intense peaks at 2θ = 36.78, 42.76 and 62.16° among which the peaks at 2θ = 42.76 and 62.16° are the most prominent. The X-ray diffraction pattern of MgO NPs suggested a highly crystalline structure of the NPs. On the other hand, the diffractogram of neat PLA films demonstrated mainly a broad peak around 2θ = 16.5°. Absence of any sharp peak indicated a completely amorphous phase of the PLA films [8, 13]. Similarly, the prepared biocomposite films also demonstrated a broad peak around 2θ = 16.5°, corresponding to PLA, suggesting a fully amorphous phase in the films [13]. In addition to the broad peak at 2θ = 16.5°, the diffractograms of biofilms consisted an increase in diffraction intensities at 2θ = 36.78, 42.76° and 62.16° corresponding to the diffraction peaks of MgO NPs, which increased with the higher loading of NPs. The peaks corresponding to PLA and MgO NPs appears at same 2θ values in all biofilms which suggested successful preparation of PLA/MgO biofilms by solvent casting process. Comparable results were also reported in previous studies [8, 13, 15]

The surface morphology of prepared films was studied by FE-SEM analysis. The primary motivation of performing FE-SEM study at the surface of the films was that

since the food will be in contact with the surface of the films rather than the cross-section [8]. The FE-SEM micrographs of the various biofilm types (P0-P4) are presented in Fig. 4.

Figure 4: FE-SEM micrographs of solvent casted films: (P0) Neat PLA, (P1) 1 wt%, (P2) 2 wt%, (P3) 3 wt% and (P4) 4 wt% PLA/MgO biofilms

The surface investigation of films revealed uniform dispersion of NPs in entire sample in form of agglomerations (seen as white dots) which increased with the loading of NPs. Investigation of film surfaces also revealed a smooth and compact surface of pristine PLA films. Nano-fillers possess high surface energy due to their tiny sizes and therefore they tend to agglomerate in order to minimize their surface energy [16, 17]. These agglomerated particles contribute to the roughness of the film surface, which has also been captured in FE-SEM analysis. The roughness of films increased with loading of MgO NPs mainly due to the increased tendency of agglomeration at higher filler loading. FE-SEM analysis of the films evidence no physical defects at the surface of films which suggests successful casting of the PLA/MgO films by solvent casting method. Similar surface morphology was also observed in previous study [8, 14]. In addition to surface morphology, dispersion of MgO NPs and composition of biofilms was also confirmed by Energy-Dispersive X-ray spectroscopy (EDX) analysis. The elemental mapping of 2 wt% PLA/MgO biofilms along with corresponding elemental composition is illustrated in Fig. 5.

Figure 5: EDX analysis of PLA/MgO film with elemental mapping in inset

It can be observed that biofilms consist of C, O and Mg elements, furthermore, the elemental mapping illustrates the uniform distribution of MgO NPs in the films.

4.2. Tensile Properties

Mechanical strength plays a vital role during the entire life cycle of any packaging, therefore, it is of vital importance to study the mechanical properties of packaging films. Key mechanical properties such as tensile strength (TS), elastic modulus (EM) and elongation at break (EAB) of the biocomposite films were determined from the plotted stress-strain curves. Typical stress-strain relationships of the films and mean values of the properties along with their range are presented in Fig. 6 (a) and (b) respectively.

Figure 6:(a) Typical stress-strain curves of prepared films and (b) Tensile properties of PLA and PLA/MgO biocomposite films

As depicted in Fig. 6, the mechanical properties of pristine PLA films improved significantly by incorporation of 1 wt% of MgO nano-filler, which could be attributed to effective stress transfer between polymer chains and nano-filler due to higher interfacial area offered by tiny NPs. Smaller size nano-fillers offer higher surface to volume ratio (inversely proportional to radius of spherical or near spherical particles) compared to relatively bigger NPs (size <100 nm) [17]. In this context, the size of nano-fillers plays a vital role in the enhancement of mechanical properties. The effectiveness of reinforcement of nano-filler is governed principally in two ways, first, addition of nano-sized fillers in polymer matrix provides relatively high surface interaction between the filler and polymer chains which facilitates enhanced stress transfer from polymer chains to nano-fillers resulting in an improvement in mechanical properties [13]. Secondly,

contrarily to first, due to high surface energy of NPs they tend to agglomerate which reduces the effective filler content in the matrix, furthermore, agglomerated particles start acting like an imperfection/ defect in the polymer network which limits the expected improvement in properties at higher filler reinforcement [8, 16, 17].

In this research TS of the biocomposite films increased up to 2 wt% loading of NPs mainly due to relatively fine and uniform dispersion of NPs in PLA matrix, further addition of the NPs led to an inferior property compared to the unfilled PLA films largely due to the agglomeration of NPs acting like a defect in samples. The TS of biofilms increased nearly by 29% for 2 wt% films, in comparison to the pristine PLA films. The improvement in TS and EM revealed a good compatibility of MgO NPs and PLA matrix. On the other hand, EAB decreased significantly owing to the fact that presence of NPs in polymer network restricts the free movement of polymer chains which consequently decreases the EAB [14]. The EAB notably decreased with reinforcement of 1 wt% NPs. Interestingly, further addition of NPs (up to 2 wt%) slightly increased EAB which could most likely ascribe to effective decrease in filler content due to agglomeration of NPs. The severity of agglomeration increased with further addition of filler which acts as a preferential location for stress concentration followed by rupture of samples during tensile pull and hence restraining further elongation [8]. In this context the 3 and 4 wt% biofilms demonstrated a lowest EAB (around 47% less compared to neat PLA films). Among the prepared films, the 2 wt% films exhibited the best tensile strength including highest EAB which can be endorsed to the uniform dispersion of NPs in the PLA matrix, as also observed in surface analysis through FE-SEM (Fig. 4). Similar improvement in tensile properties was also reported in other studies [13, 18].

4.3. Thermal Properties

Thermal properties, like degree of crystallinity (%χ), glass transition temperature (T_g) and melting temperature (T_m) were determined by DSC analysis. Thermograms of the second heat cycle of DSC scans are illustrated in Fig. 7 and the computed thermal properties are summarized in Table 1.

Figure 7: DSC thermograms of biocomposite films: (P0) Neat PLA, (P1) 1 wt%, (P2) 2 wt%, (P3) 3 wt% and (P4) 4 wt% PLA/MgO biofilms

The degree of crystallinity of the films was determined using the following relation [19]:

$$\%\chi = [\Delta H_m - \Delta H_c / \Delta H_m^o] \times 100$$

where ΔH_m is the melting enthalpy of sample, ΔH_c is the cold crystallization enthalpy and ΔH°_m is the theoretical melting enthalpy of 100% crystalline PLA, which is equivalent to 93 J/g. The DSC scans highlighted that ΔH_c is slightly higher than ΔH_m for all the films which, from the above relation, reveals no crystalline phase in crystal structure of films. From the obtained values of crystallinity, it can well be concluded that the produced biofilms consisted 100% amorphous crystal structure, which is also consistent with results of XRD analysis (Fig. 3). Furthermore, addition of MgO NPs had no notable effect on the T_g or crystallinity of the films. Similar results were also reported by [18].

Thermal stability of PLA and its biofilms was determined using the TGA technique. The TGA thermograms and derivative of TGA (DTGA) curves are shown in Fig. 8 and the values of thermal properties, such as initial decomposition temperature (IDT),

maximum rate of decomposition temperature (MRDT) and weight loss (WL) are listed in Table 1.

Figure 8: TGA and DTGA graphs of the prepared films: (P0) Neat PLA, (P1) 1 wt%, (P2) 2 wt%, (P3) 3 wt% and (P4) 4 wt% PLA/MgO biofilms

Table 1: Thermal properties of PLA and PLA/MgO biofilms

The initial weight loss between 80°C to 140°C in all the samples corresponds to the loss of moisture. Subsequently, pristine PLA films demonstrated a weight loss of 98.87% between 312°C to 402°C, mainly due to loss of the ester group during depolymerization at elevated temperature [20]. Whereas, PLA/MgO biofilms exhibited a weight loss of up to 97.7% between two distinguished temperatures ranges, 246°C to 335°C and 422°C to 490°C, respectively, due to thermo-degradation of polymer chains close to NPs and away from them [21]. The TGA analysis reveals that addition of MgO NPs in PLA matrix leads to a lower thermal stability, which is directly proportional to the amount of nano-filler added. Similar results have also been reported by other authors [13, 20].

4.4. Barrier properties

Tiny substances such as moisture, gas molecules and microorganisms that are permeable to polymer films may cause degradation of foodstuffs by microbial growth, therefore, in case of food packaging low permeability is desired. Barrier properties play a very important role in the determination of shelf life of packed food. Henceforth, oxygen and water vapour transport properties of key selected biofilms were examined. The values of oxygen permeability (OP) of the films are summarized in Table 2.

Table 2: Oxygen and water vapor permeability values of PLA and PLA/MgO biocomposite films

The PLA films prepared in this study exhibited higher oxygen transmission rate in comparison to analogous studies [8, 19]. This is most likely due to the formation of free volumes created by evaporation of the solvent in the solvent casting process which, in turn, facilitates an unrestricted space for easy diffusion of gas molecules [21, 22]. Presence of impermeable nano-fillers in polymer network affects diffusion of permeating molecules by providing hindrance to their path which results as improved barrier properties. On the way to diffuse thorough films containing nano-fillers the permeating molecules must bypass these nano-fillers which significantly elongates the mean permeation path through the torturous pathway mechanism [22, 23]. Reinforcement of MgO NPs significantly improved the oxygen barrier property of prepared films. Addition of 1 wt% MgO NPs reduced the permeability of O_2 molecules by nearly 22% in comparison to neat PLA films. The OP values decreased up to 2 wt% reinforcement of NPs, further addition of nano-filler led to inferior oxygen barrier properties. This depreciation in barrier property at higher wt% addition can be attributed to free volume region created at the interface of agglomerated NPs and polymer matrix. These free volume regions around the NPs results in a preferential path for permeation which consequently supports a relative easy diffusion of gaseous molecules compared to unfilled polymer matrix [23, 24]. Among the prepared biofilms, the 2 wt% films demonstrated a maximum decrease in OP (up to 25%) in comparison to neat PLA films. A similar decrease in gas permeability was reported in previous studies [8, 19].

Water vapor permeability of PLA and its biocomposite films were found out and are shown in Table 2. Similar to gas permeability, pristine PLA films exhibited higher permeability to water vapour also. Additionally, contrary to gas permeability, reinforcement of MgO NPs further increased the WVP. The 1 wt% films demonstrated a 20% increase in WVP when compared to neat PLA films. Generally, it is believed that addition of impermeable filler improves the barrier properties of films by altering the path of permeants. However, permeability of water vapor (polar molecule) is not governed merely by the torturous pathway effect. Instead the modification of absorption and solubility at interface and free volume regions near NPs collectively contribute to an increase in the permeability [8, 22, 23]. Congruent WVP behavior of PLA/ZnO films was reported in another study [8].

4.5. Antibacterial properties

Metal oxides possess superior antibacterial efficacy [8]. Their reinforcement in polymers significantly improves bactericidal properties of the films, which is desired in food packaging applications. However, verification of its retention in form of biofilms is necessary. Considering the improved mechanical and barrier properties of 2 wt% PLA/MgO biofilms, its antibacterial efficacy was studied in comparison to pristine PLA films against the foodborne bacteria, E. Coli. The FACS results are presented in Fig. 9 in terms of dot plots between fluorescence intensities of detectors (FL1 and FL2) after incubation of propidium iodide, used primarily for staining of damaged membranes of E. Coli cells [25].

Figure 9:Flow cytometry dot plots of (a) pristine PLA films and (b) treatment with 2 wt% biofilms for 12 h

Shifting of fluorescence intensities from the first quadrant to other confirmed death of the bacteria. Around 46% of E. Coli cells lead to damage and death upon treatment of 2 wt% PLA/MgO films for 12 h which in turn confirmed retainment of superior antibacterial efficacy of MgO NPs reinforced in PLA matrix. Comparable results are also reported in [8].

5. Conclusions

This study was focused on incorporation of MgO NPs in PLA matrix and examination of key properties of prepared biofilms for food packaging applications. The structural and chemical adequacy of solvent casted films was evaluated by XRD, FTIR and FE-SEM techniques. XRD and DSC analysis revealed a highly amorphous structure of the films and incorporation of MgO NPs had no significant effect on their crystallinity. The FTIR investigation did not observe any chemical bond between MgO NPs and PLA matrix which confirmed successful formation of biocomposite films. FE-SEM and EDX analysis revealed uniform distribution of MgO NPs, which was further reflected as improved mechanical and gas barrier properties. Size of dispersed phase of NPs plays a fundamental role in tailoring the overall properties of bio/nano-composites films. In this context the effect of size of nano-particle on the properties of the developed material can be studied in the future. Furthermore, the developed biofilms for prolonging shelf life of highly perishable food-stuffs such as exotic fruits and dairy products can be attempted in future work. Although both PLA and MgO used in present biofilms are recognized by

FDA for food and drug applications, toxicity/compatibility tests prior to any real-life application are also recommended. Overall, considering the lower cost of MgO NPs compared to other metal oxides and improved tensile and gas barrier properties augmented with improved antibacterial efficacy and UV screening ability, it can be said that incorporation of MgO in PLA matrix appears to be a very promising approach for developing a novel material for food packaging applications.

Acknowledgements

The authors would like to acknowledge the testing and characterization facilities of the Centre for Interdisciplinary Research (CIR) and Department of Applied Mechanics, MNNIT, Allahabad. The authors are also grateful to Advanced Imaging Centre, IIT Kanpur, Defence Materials and Stores Research and Development Establishment, Kanpur, Laboratory for Advanced Research in Polymeric Materials, CIPET, Bhubaneshwar, India and Polymer Processing Research Centre, Queen's University Belfast, U.K. for extending their research facilities. The lead author would like to thank the Ministry of Human Resource Development, Government of India for providing financial support.

References

1. V. Siracusa, P. Rocculi, S. Romani, and M. D. Rosa, Biodegradable polymers for food packaging: a review, Trends Food Sci. Technol. 19 (2008) 634–643
2. J. M. Raquez, Y. Habibi, M. Murariu, and P. Dubois, Polylactide (PLA)-based nanocomposites, Prog. Polym. Sci. 38 (2013) 1504–1542

3. R. Y. Tabasi, Z. Najarzadeh, and A. Ajji, Development of high performance sealable films based on biodegradable/compostable blends, Ind. Crops Prod. 72 (2015) 206–213
4. A. M. Youssef, Polymer Nanocomposites as a New Trend for Packaging Applications, Polym. Plast. Technol. Eng. 52 (2013) 635–660
5. L. J. Chan, O. M. Feeney, N. J. Leong, V. M. Mcleod, C. J. H. Porter, C. C. Williams and L. M. Kaminskas, An Evaluation of Optimal PEGylation Strategies for Maximizing the Lymphatic Exposure and Antiviral Activity of Interferon after Subcutaneous Administration. (2017) https://doi.org/10.1021/acs.biomac.7b00794
6. Z. Fan, Z. Xu, H. Niu, N. Gao, Y. Guan, C. Li, Y. Dang, X. Cui, X. L. Liu, Y. Duan, H. Li, X. Zhou, P. H. Lin, J. Ma and J. Guan, An Injectable Oxygen Release System to Augment Cell Survival and Promote Cardiac Repair Following Myocardial Infarction. Scientific Reports, 8:1371 (2018), https://doi.org/10.1038/s41598-018-19906-w
7. J. Ahmed, M. Z. Mulla, Y. A. Arfat, Thermo-mechanical, structural characterization and antibacterial performance of solvent casted polylactide/cinnamon oil composite films, Food Control, 69 (2016) 196–204
8. A. Marra, C. Silvestre, D. Duraccio, S. Cimmino, Polylactic acid/zinc oxide biocomposite films for food packaging application, Int. J. Biol. Macromol. 88 (2016) 254–262
9. S. Sanuja, A. Agalya, M. J. Umapathy, Studies on magnesium oxide reinforced chitosan bionanocomposite incorporated with clove oil for active food packaging application, Int. J. Polym. Mater. Polym. Biomater. 63 (2014) 733–740

10. C. Swaroop, M. Shukla, Polylactic acid/ magnesium oxide nanocomposite films for food packaging applications, Proceedings of 21st International Conference on Composite Materials. Xi'an, China. 20-25 August 2017, Paper ID 3695
11. A. Das M. Shukla, Surface morphology, bioactivity, and antibacterial studies of pulsed laser deposited hydroxyapatite coatings on Stainless Steel 254 for orthopedic implant applications, Proc. Inst. Mech. Eng. Part L J. Mater. Des. Appl. (2016) https://doi.org/10.1177/1464420716663029
12. R. Auras, L. T. Lim, Susan E. M. Selke, H. Tsuji, Poly (lactic acid) Synthesis, Structures, Properties, Processing, and Applications, John Wiley and Sons, Inc. 2010
13. J. Jayaramudu, K. Das, M. Sonakshi, G. Siva Mohan Reddy, B. Aderibigbe, R. Sadiku, S. Sinha Ray, Structure and Properties of Highly Toughened Biodegradable polylactide/ZnO Biocomposite Films, Int. J. Biol. Macromol 64 (2014) 428–34
14. J. Ahmed, Y. A. Arfat, E. Castro-Aguirre, R. Auras, Mechanical, structural and thermal properties of Ag-Cu and ZnO reinforced polylactide nanocomposite films, Int. J. Biol. Macromol. 86 (2016) 885–892
15. R. Pantani, G. Gorrasi, G. Vigliotta, M. Murariu, P. Dubois, PLA-ZnO nanocomposite films: Water vapor barrier properties and specific end-use characteristics, Eur. Polym. J. 49 (2013) 3471–3482
16. S. Mishra, S. H. Sonawane, R. P. Singh, A. Bendale, and K. Patil, Effect of Nano-$Mg(OH)_2$ on the mechanical and flame-retarding properties of polypropylene composites, J. Appl. Polym. Sci. 94 (2004) 116–122.
17. A. J. Crosby and J. Lee, Polymer Nanocomposites: The 'Nano' Effect on Mechanical Properties, Polym. Rev. 47 (2007) 217–229.

18. S. Girdthep, N. Komrapit, R. Molloy, S. Lumyong, W. Punyodom, P. Worajittiphon, Effect of plate-like particles on properties of poly(lactic acid)/poly(butylene adipate-co-terephthalate) blend: A comparative study between modified montmorillonite and graphene nanoplatelets, Compos. Sci. Technol. 119 (2015) 115–123
19. H. D. Huang, P. G. Ren, J. Chen, W. Q. Zhang, X. Ji, Z. M. Li, 'High barrier graphene oxide nanosheet/poly(vinyl Alcohol) nanocomposite films', J. Memb. Sci. 464 (2014) 110–118
20. I. Restrepo, N. Benito, C. Medinam, R. V Mangalaraja, P. Flores, S. Rodriguez-Llamazares, Development and characterization of polyvinyl alcohol stabilized polylactic acid/ZnO nanocomposites, Mater. Res. Express 4 (2017) 105019
21. A. M. Pinto, J. Cabral, D. A. P. Tanaka, A. M. Mendes, F. D. Magalhaes, Effect of incorporation of graphene oxide and graphene nanoplatelets on mechanical and gas permeability properties of poly(lactic acid) films, Polym. Int. 62 (2013) 33–40
22. L. E. Nielsen, Models for the Permeability of Filled Polymer Systems, J. Macromol. Sci. Part A - Chem. 1 (1967) 929–942
23. T. V. Duncan, Applications of nanotechnology in food packaging and food safety: Barrier materials, antimicrobials and sensors, J. Colloid Interface Sci. 363 (2011) 1–24
24. M. Abdollahi, M. Alboofetileh, R. Behrooz, M. Rezaei, R. Miraki, Reducing water sensitivity of alginate bio-nanocomposite film using cellulose nanoparticles, Int. J. Biol. Macromol. 54 (2013) 166–173

25. A. Paparella, L. Taccogna, I. Aguzzi, C.C. Lopez, A. Serio, F. Marsilio, G. Suzzi, Flow cytometric assessment of the antimicrobial activity of essential oils against Listeria monocytogenes, Food Control, 19 (2008) 1174–1182

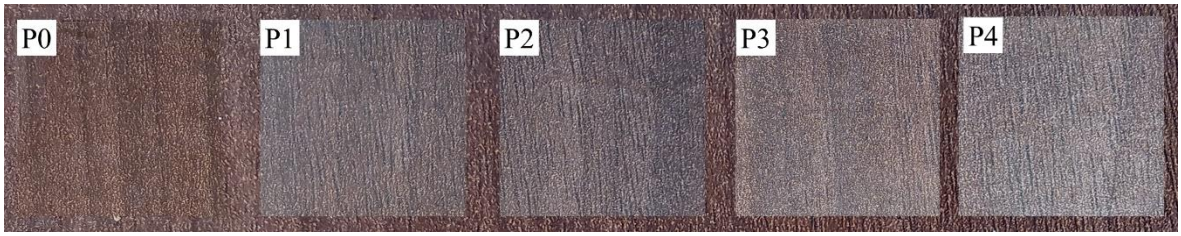

Figure 1: Different types of prepared biofilms: (P0) Neat PLA, (P1) 1 wt%, (P2) 2 wt%, (P3) 3 wt% and (P4) 4 wt% PLA/MgO biofilms

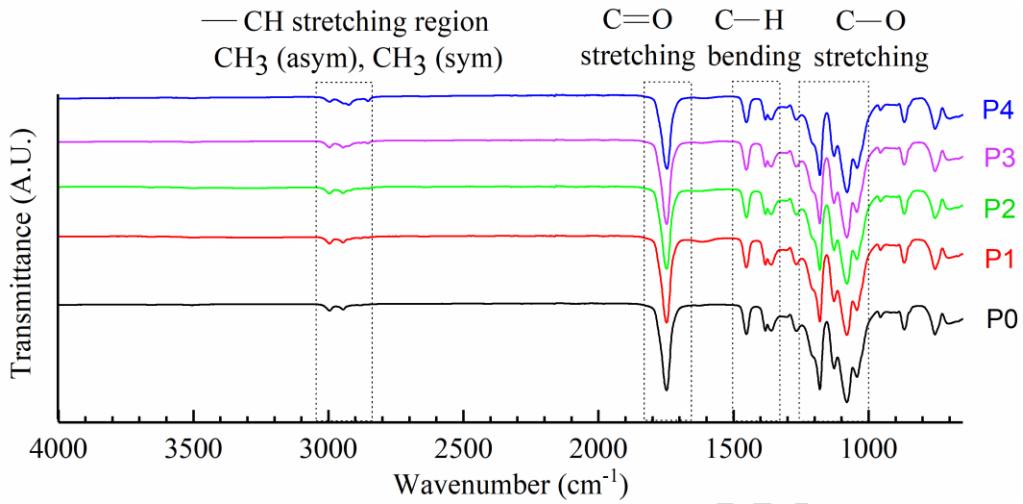

Figure 2: FTIR spectra of prepared films: (P0) Neat PLA, (P1) 1 wt%, (P2) 2 wt%, (P3) 3 wt% and (P4) 4 wt% PLA/MgO biofilms

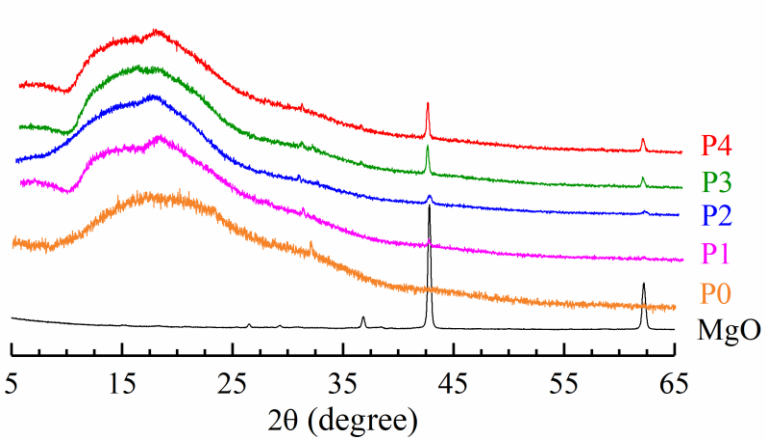

Figure 3: XRD diffractograms of MgO NPs and prepared biocomposite films: (P0) Neat PLA, (P1) 1 wt%, (P2) 2 wt%, (P3) 3 wt% and (P4) 4 wt% PLA/MgO biofilms

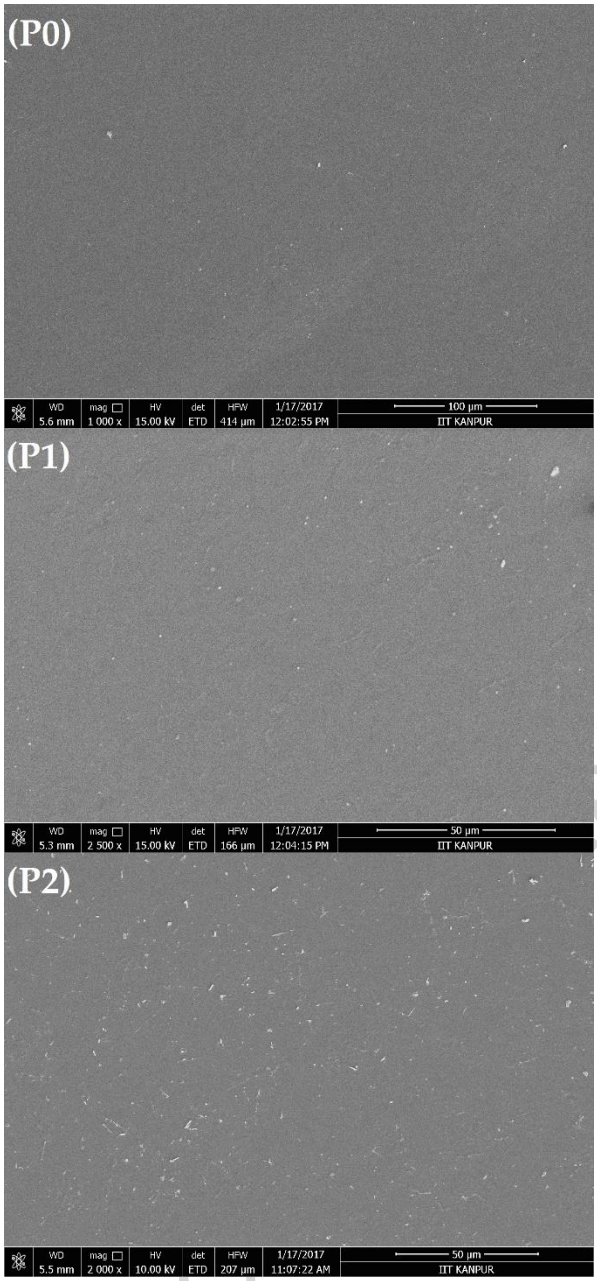

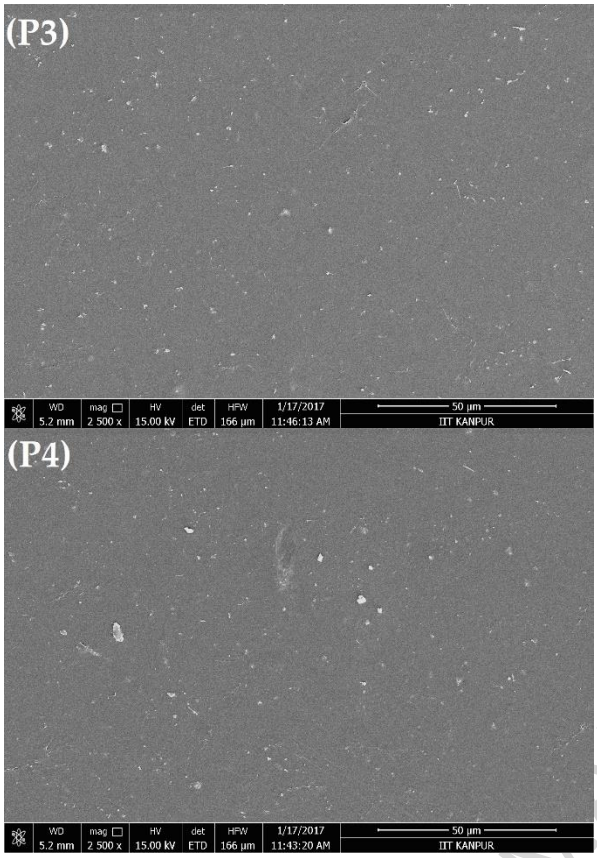

Figure 4: FE-SEM micrographs of solvent casted films: (P0) Neat PLA, (P1) 1 wt%, (P2) 2 wt%, (P3) 3 wt% and (P4) 4 wt% PLA/MgO biofilms

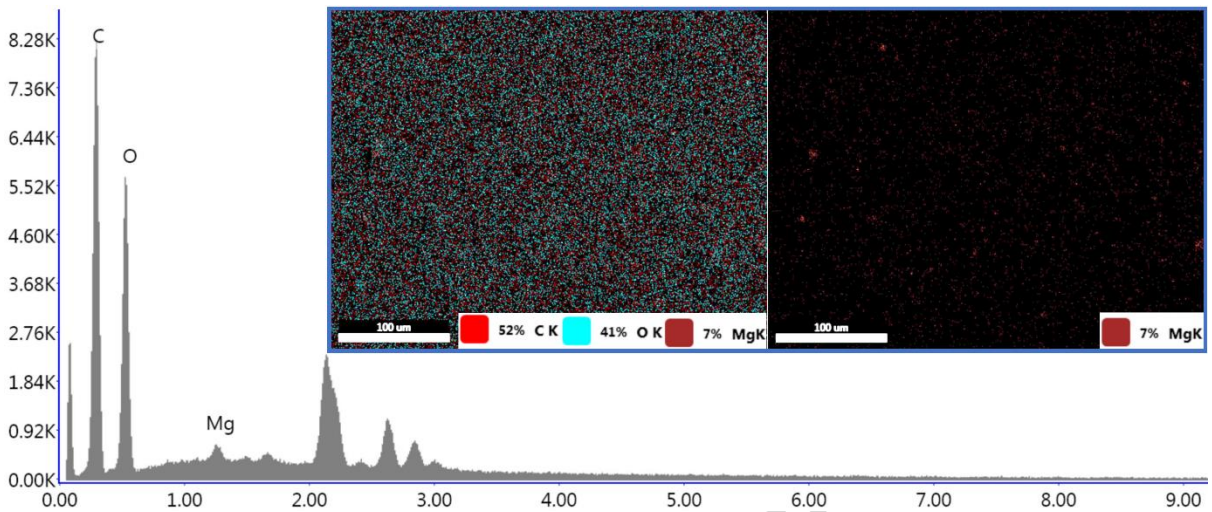

Figure 5: EDX analysis of PLA/MgO film with elemental mapping in inset

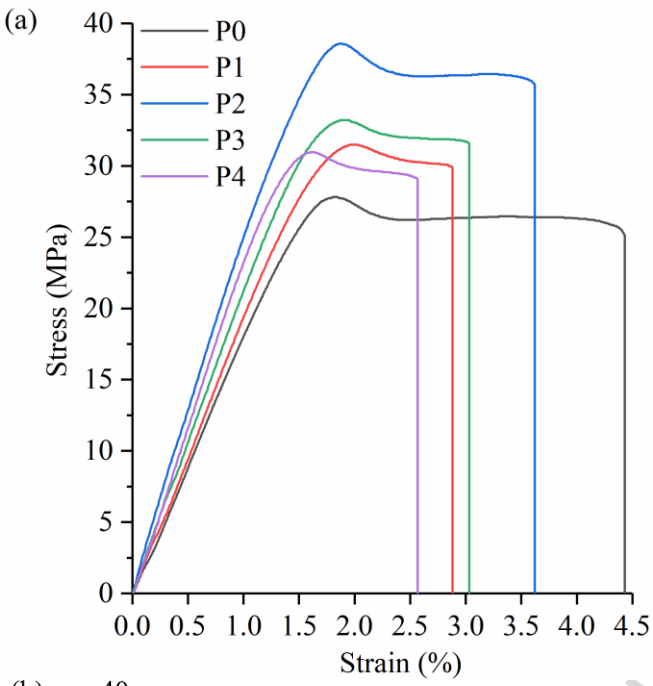

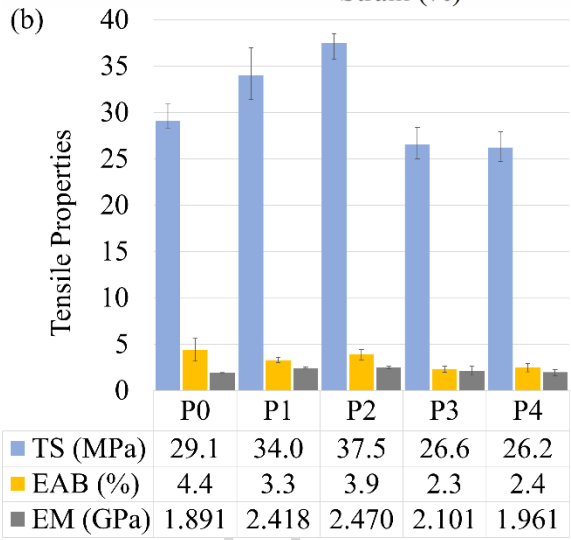

	P0	P1	P2	P3	P4
TS (MPa)	29.1	34.0	37.5	26.6	26.2
EAB (%)	4.4	3.3	3.9	2.3	2.4
EM (GPa)	1.891	2.418	2.470	2.101	1.961

Figure 6: (a) Representative stress-strain curves of prepared biocomposite films and (b) Tensile properties of prepared films

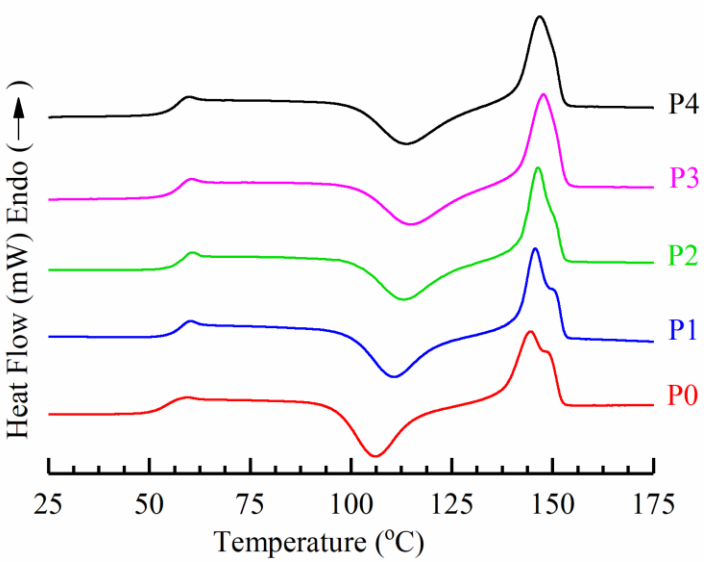

Figure 7: DSC thermograms of biocomposite films: (P0) Neat PLA, (P1) 1 wt%, (P2) 2 wt%, (P3) 3 wt% and (P4) 4 wt% PLA/MgO biofilms

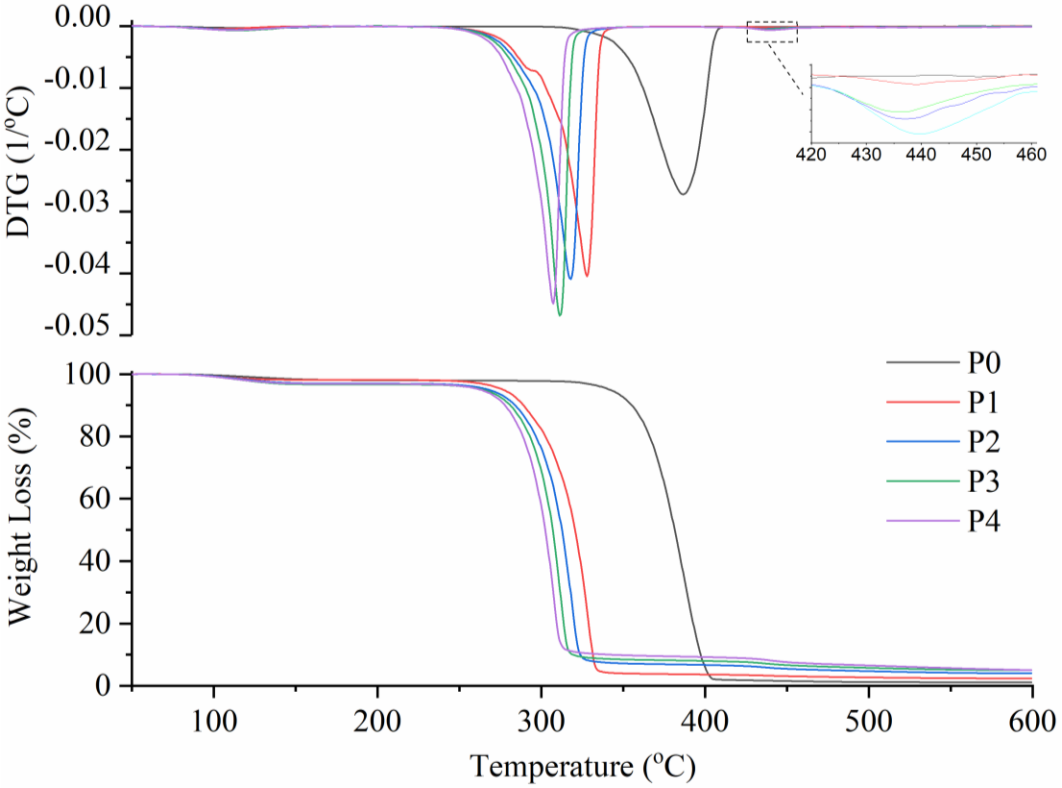

Figure 8: TGA and DTGA graphs of the prepared films: (P0) Neat PLA, (P1) 1 wt%, (P2) 2 wt%, (P3) 3 wt% and (P4) 4 wt% PLA/MgO biofilms

(a)

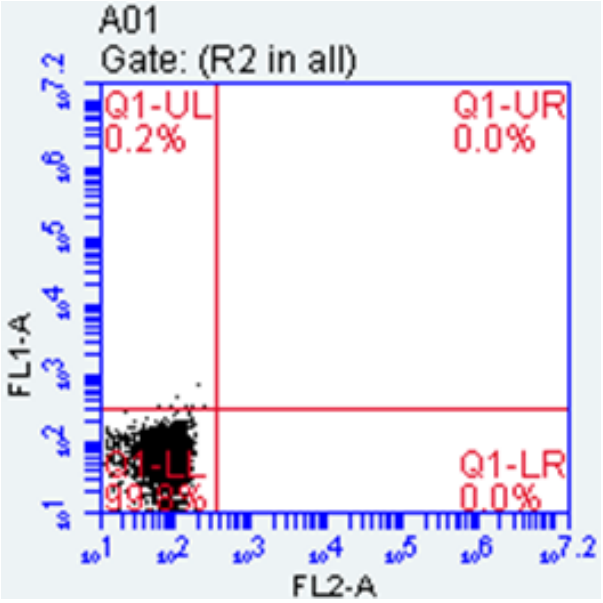

(b)

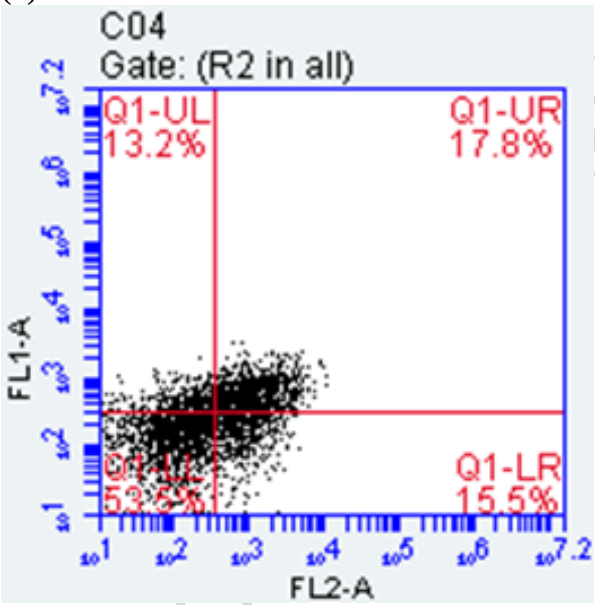

Figure 9: Flow cytometry dot plots of (a) control (pristine PLA films) and (b) treatment with 2 wt% PLA/MgO biofilms for 12 h

Table 1: Thermal properties of PLA and PLA/MgO biofilms

Sample	DSC					TGA		
	T_g (^{O}C)	T_c (^{O}C)	ΔH_c (J/g)	T_m (^{O}C)	ΔH_m (J/g)	IDT (^{O}C)	$MRDT$ (^{O}C)	WL (%)
Neat PLA films (P0)	58.09	105.77	21.02	146.56	19.09	353.82	386.53	98.87
1 wt% PLA/MgO biofilms (P1)	57.34	110.64	22.81	145.71	22.57	291.97	327.94	97.70
2 wt% PLA/MgO biofilms (P2)	57.98	120.93	19.76	148.19	18.94	288.35	317.88	95.89
3 wt% PLA/MgO biofilms (P3)	57.29	114.90	43.31	147.73	42.81	289.87	311.56	96.39
4 wt% PLA/MgO biofilms (P4)	57.53	113.57	35.52	146.86	34.05	279.71	307.34	96.39

Table 2: Oxygen and water vapor permeability values of PLA and PLA/MgO biocomposite films

Sample	OP (cm^3/m^2 day) × (mm/kPa)	WVP (× 10^{-13} g/m^2 sec) × (m/Pa)
Neat PLA films (P0)	7.53	5.09
1 wt% PLA/MgO biofilms (P1)	5.85	7.22
2 wt% PLA/MgO biofilms (P2)	5.66	6.38
4 wt% PLA/MgO biofilms (P4)	7.38	8.79